

Absorption Wavelength Extension for Dye-Sensitized Solar Cells by Varying the Substituents of Chiral Salen Cu(II) Complexes

Ryosuke Shoji¹, Shun Ikenomoto¹, Nobumitsu Sunaga¹, Mutsumi Sugiyama² and Takashiro Akitsu^{1,*}

¹Department of Chemistry, Faculty of Science, Tokyo University of Science, 1-3 Kagurazaka, Shinjuku-ku, Tokyo 162-8601, Japan

²Department of Electrical Engineering, Faculty of Science and Technology, Tokyo University of Science, 2641 Yamazaki, Noda, Chiba 278-8510, Japan

Abstract: New chiral salen-type Cu(II) complexes (**1-9**) were prepared, and the effects of different substituent groups on their absorption spectra were evaluated using time-dependent density functional theory (TD-DFT). Electron withdrawing groups resulted in a red-shift and an increase in the peak intensity. According to cyclic voltammetry analyses, the introduction of electron withdrawing groups brought the redox potentials (E^0) in agreement with the orbital level energies determined via TD-DFT. The reduction potentials for **1-9** are less than -0.500 V, and therefore, it is electrochemically possible to dope electrons in TiO_2 . In addition, the oxidation potentials are greater than $+0.200$ V, indicating that it is electrochemically possible to regenerate the dyes. Preproduction dye-sensitized solar cells (DSSCs) fabricated using compounds **1-9** generated electricity. In particular, the DSSC prepared using **2** (which has electron withdrawing groups and the largest maximum absorption) exceeded the power conversion efficiency of DSSC fabricated using **N3**, which is a commonly used Ru(II) complex.

Keywords: DSSC, Copper(II), Schiff base, Chirality, Crystal structure.

INTRODUCTION

Various mechanisms to provide improved current generation efficiencies in dye-sensitized solar cells (DSSCs) have been devised [1-7]. Recently, the power conversion efficiencies (PCEs) of DSSCs have improved due to the use of new photosensitisers such as Ru(II) complexes. To further improve the PCE of DSSCs, however, it is necessary to find dyes that absorb photons efficiently over the entire visible and near-infrared (NIR) regions. The compound **N719** ($[\text{RuL}_2(\text{NCS})_2]:2\text{TBA}$; $\text{L}=2,2'$ -bipyridyl-4,4'-dicarboxylic acid, TBA = tetra-*n*-butyl ammonium) is known to achieve photoelectric conversion to 900 nm [8]. However, **N719** is susceptible to degrade through the dissociation of its labile NCS^- ligands. Therefore, to improve the dye stability, the replacement of the NCS^- ligands with chelating ligands such as naphthalimide, porphyrin Zn(II) complexes or phthalocyanine Cu(II) complexes, has been investigated [9, 10].

Dyes have also been shown to adsorb on TiO_2 surface via interaction with the $\text{Ti}2p$ and $\text{O}1s$ orbitals of their carboxy groups [11]. However, dyes such as **N719** and **N3** ($\text{RuL}_2(\text{NCS})_2$; $\text{L}=2,2'$ -bipyridyl-4,4'-dicarboxylic acid), which contain NCS^- ligands, adsorb on TiO_2 via the interactions of their S atoms. Therefore, the control

of the adsorption structure via co-adsorption has been reported [12].

Our focus has been on salen metal complexes because they have the following characteristics:

- (1) Their synthesis and chemical modification are easier than what is required for existing dyes.
- (2) They have higher stability than existing dyes due to the presence of chelating ligands.
- (3) They have various interesting magnetic and optical properties and oxidation–reduction reactivities due to their electron transfer behaviour.
- (4) They are known to catalyse asymmetric synthesis and redox reactions [13, 14].

Therefore, salen metal complexes have potential for use as dyes in DSSCs. Increasing the PCE of salen Zn(II) complexes by varying the substituents has been reported [15]. In addition, the UV–vis spectra of salen Al(III) complexes were found to be red-shifted following the incorporation of electron-withdrawing substituents [16]. It is therefore expected that substituent effects in salen metal complexes should be useful for controlling absorption across the visible and NIR regions as well as E^0 values.

It is also known that the interactions between chiral molecules and nanoparticles or semiconductors

*Address correspondence to this author at the Department of Chemistry, Faculty of Science, Tokyo University of Science, 1-3 Kagurazaka, Shinjuku-ku, Tokyo 162-8601, Japan; Tel: +81-3-5228-8271; E-mail: akitsu@rs.kagu.tus.ac.jp

produce new circular dichroism (CD) signals due to dipole interactions and dielectric effects [17, 18]. Thus, the interaction of chiral salen metal complexes with TiO_2 should result in the expansion of the wavelength region over which these complexes absorb light, which is conventional but effective strategy.

To design DSSC dyes, we therefore investigated the effect of the different substituents in Cu(II) salen complexes **1-9**, involving common metal Cu(II), on the

shift of their absorbances to the NIR region and their reduction potentials (Figure 1). The performance of DSSC devices based on the complexes was also achieved and compared to that of a DSSC based on **N3**.

RESULTS AND DISCUSSION

As shown in Figure 1, **1** is a five-coordinated mononuclear Cu(II) complex with a square pyramidal

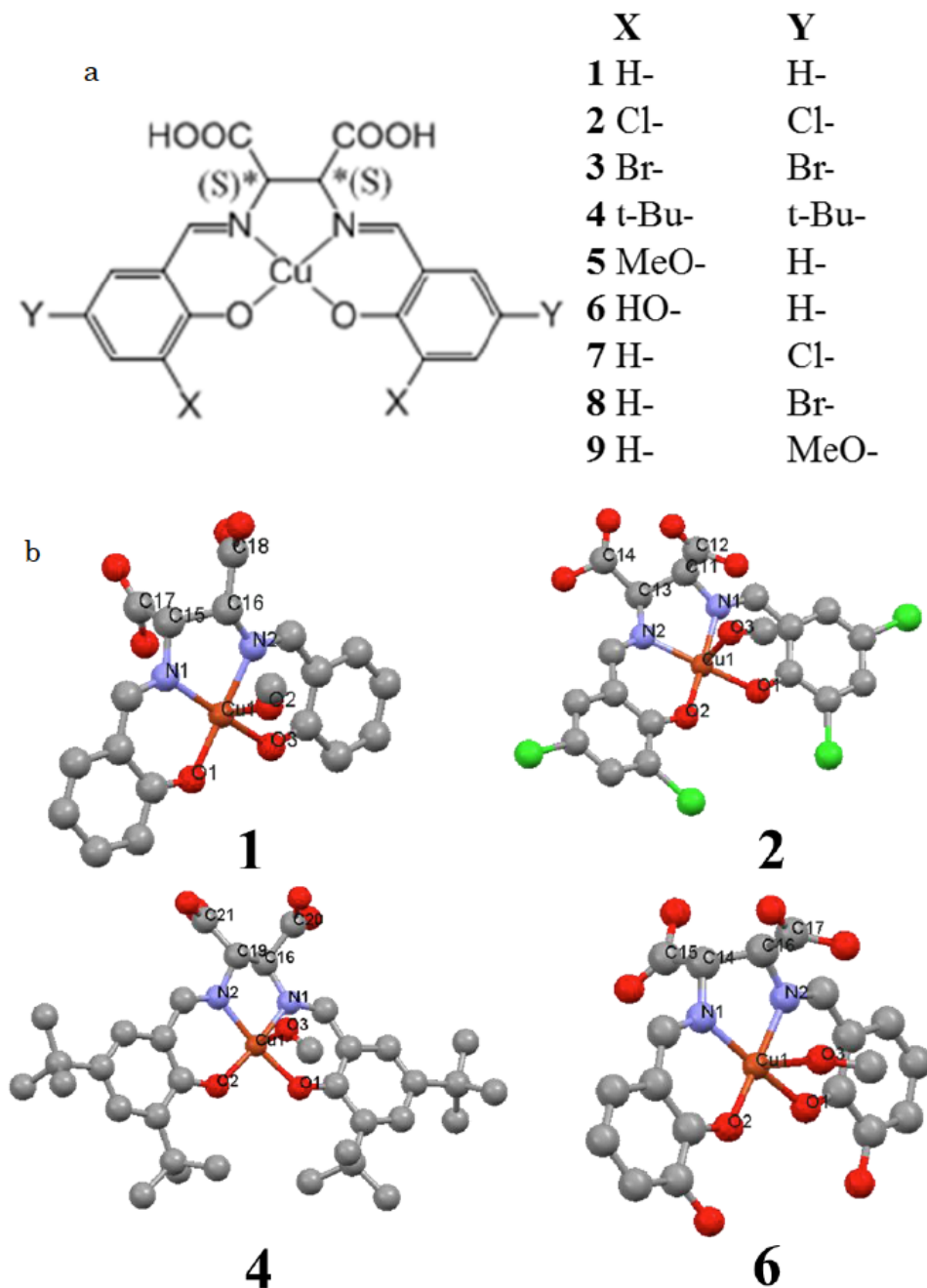


Figure 1: (a) Chiral salen Cu(II) complexes **1-9** and (b) molecular structures of **1**, **2**, **4** and **6**. Hydrogen atoms are omitted for clarity.

[CuN₂O₃] geometry. The four donor atoms of the tetradentate Schiff base form the equatorial plane, and MeOH ligands occupy the axial sites with the Cu1-O1, Cu1-O3, Cu1-N1 and Cu1-N2 bond distances ranging from 1.9141(5) to 2.0711(5) Å and the Cu1-O2 bond distance for the axial O atom of 2.0491(5) Å (Table 1). The chiral (2*S*,3*S*)-3-aminoaspartic acid moiety adopts a λ configuration. Structures of **2**, **4** and **6** are summarised in Tables **S1-S4**.

The torsion angles of complexes **1**, **2**, **4** and **6** may be affected by the electron donating groups of the two substituents (X-). In particular, the contortion of the torsion angle is thought to be due to the repulsion of the electrons of the carboxy groups qualitatively. Thus, because the complexes should interact with TiO₂ through the carboxy groups, the changes in the torsion angles due to the substituents should affect the distance between each adsorbed complex and TiO₂, which in turn should influence their current density–voltage (*J*–*V*) properties.

Figures **2a** and **b** depict the UV–vis–NIR and CD spectra (solid state and DMF solutions, respectively)

for complexes **1-9**. A comparison of the UV–vis–NIR spectra of the complexes revealed the role of the substituents in the salen ligand. It can be clearly seen that the π – π^* absorbance bands in the diffuse reflectance electronic spectra were red-shifted in the order **7** > **9** > **3** > **5** > **2** > **4** > **8** > **6** > **1**. These results indicate that the Cu(II) complexes containing two substituents (Y-) and electron withdrawing groups had more significantly red-shifted peaks. The large difference in the red-shifts for the peaks for complexes **8** and **7**, which have Br- and Cl- substituents, respectively, can be attributed to the difference in the electronegativities of Cl and Br. Therefore, the red-shift of the π – π^* band increased when the complexes contained two substituents (Y-) and/or the substituent was an electron withdrawing group with a high electronegativity. In addition, the d–d bands in the diffuse reflectance electronic spectra of the complexes were red-shifted in the order **2** > **4** > **9** > **7** > **3** > **5** > **1** > **8** > **6**. The results also indicate that the incorporation of ligands in the Cu(II) complexes with electron withdrawing groups contributed significantly to the red-shift. For example, the d–d band for complex **5**(X-) was

Table 1a: Crystallographic Data for 1

Empirical formula	C ₁₉ H ₁₈ CuN ₂ O ₇
Formula weight	449.90
Crystal system	Monoclinic
Space group	<i>P</i> 2 ₁ / <i>n</i> (#14)
<i>a</i> (Å)	14.3880 (5)
<i>b</i> (Å)	18.7418 (18)
<i>c</i> (Å)	13.2804 (16)
β (°)	91.358 (9)
<i>V</i> (Å ³)	3580 (2)
<i>Z</i>	4
Rwp (%)	15.53

Table 1b: Selected Bond Lengths and Angles for 1

Cu 1 - O 1	1.9141(5)Å	O 1 - Cu 1 - O 3	92.07(3)°
Cu 1 - O 2	2.0491(5)Å	O 1 - Cu 1 - N 1	91.44(3)°
Cu 1 - O 3	1.9869(5)Å	O 1 - Cu 1 - N 2	170.6731(15)°
Cu 1 - N 1	2.0711(5)Å	O 2 - Cu 1 - N 1	89.25(2)°
Cu 1 - N 2	2.0002(5)Å	O 3 - Cu 1 - N 1	172.365(2)°
		O 3 - Cu 1 - N 2	93.52(3)°
		N 1 - Cu 1 - N 2	83.91(3)°

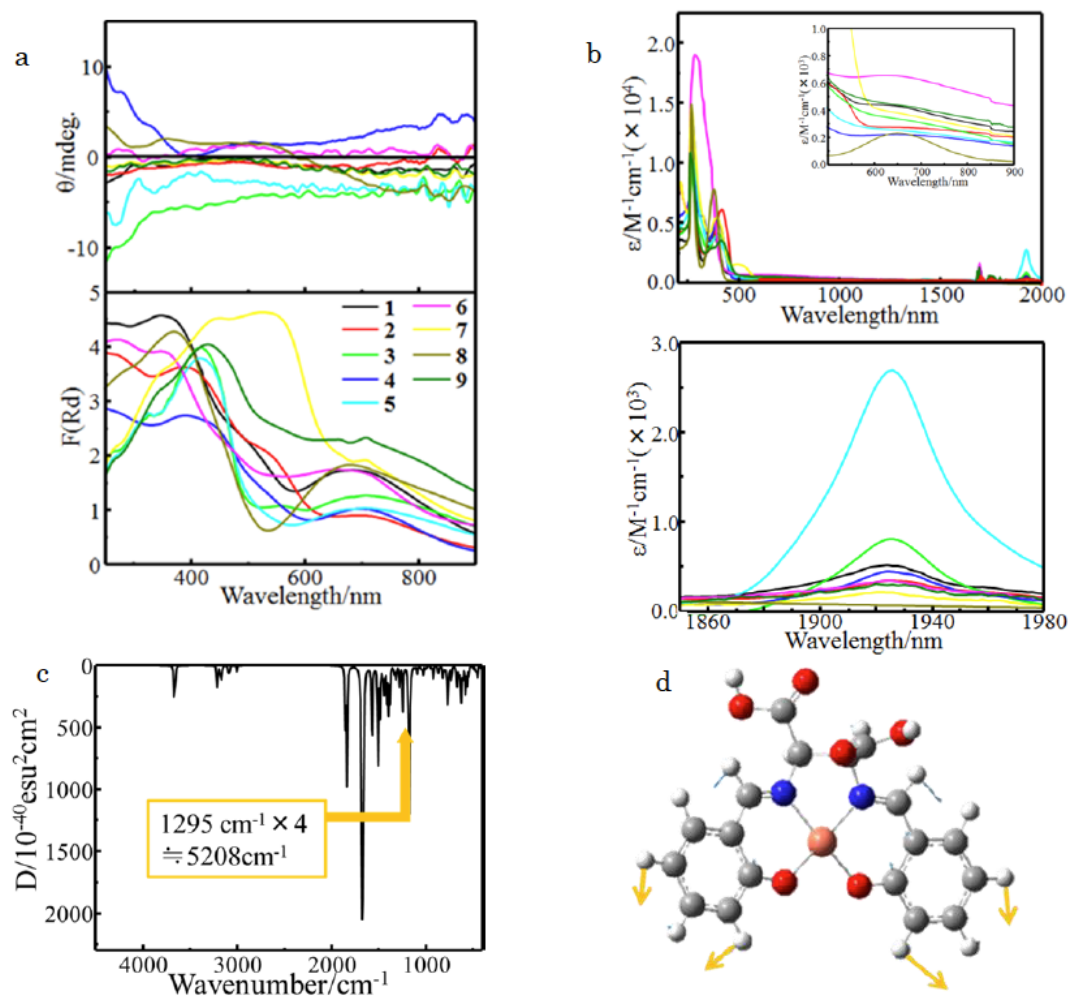


Figure 2: UV-vis-NIR and CD spectra of complexes **1-9** in the (a) solid state and (b) DMF solution, (c) calculated IR spectra of **1** and (d) normal vibrations of **1**.

red-shifted much more significantly than that for complex **9**(Y-). Therefore, it can be concluded that the incorporation of an electron withdrawing substituent at position X- has a large effect on the red-shift of the d-d band in these Cu(II) salen complexes. The correlation mainly mentions not slight difference of electronegativity of substituent groups but the number of electron-withdrawing groups. We thought that NIR band contribute vibronic coupling to absorb UV light which directly occurs photo-induced electron transfer. In general dye complexes of DSSC adsorb chemically onto (Lewis acidic) TiO₂ as deprotonated form. We assumed protonated form of the complexes as this model.

The absorption intensities of the π - π^* transitions for all the complexes **1-9** were in the range of 10^4 , and as the absorption wavelength shifted due to the incorporation of electron withdrawing groups, the intensity increased. Conversely, the absorption intensities of the d-d transitions were of the order of

10^2 , and the influence of the electron withdrawing substituents was less than that observed for the π - π^* transitions. Note that the absorption at approximately 1900 nm had an intensity of the order of 10^3 for all the complexes. Complex **5**, in particular, exhibited a striking change in intensity for this peak, as can be seen in Figure **2b**. These absorptions near 1900 nm are attributed to the vibrations of overtone effects (Figures **2c** and **d**).

To rationalise the importance of the molecular electronic structures associated with the X- and Y-groups in **1-9**, simulated UV-vis and CD spectra and the molecular orbitals of the ground and excited states were calculated for each, and the results for **1** are shown in Figures **3a-c**, respectively.

The electron transfer data for all the chiral salen Cu(II) complexes **1-9** when adsorbed on TiO₂ are provided in Table **S5**. In complexes **1** and **6**, the predominant absorption bands were assigned as

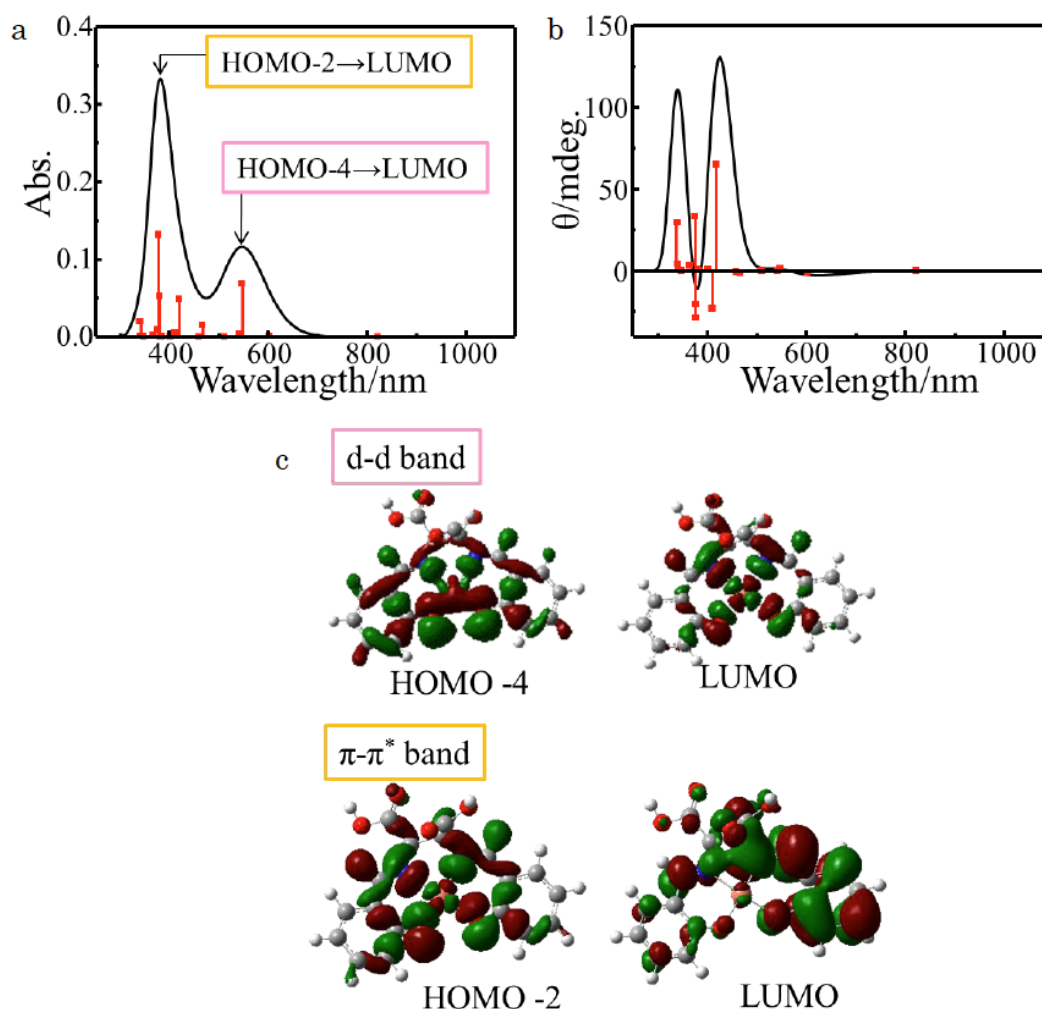


Figure 3: (a) Simulated UV-vis spectra, (b) simulated CD spectra and (c) molecular orbitals for the ground state (HOMO) and excited state (LUMO) of **1**.

transitions from the highest occupied molecular orbital (HOMO-4) to the lowest unoccupied molecular orbital (LUMO), which is distributed on the amine moieties. Based on these results, it is reasonable to conclude that the spectral shifts were due to the substitution of the X- and Y- groups. The electron transfer in all the complexes **1-9** occurred first to the aldehyde, then to the central metal and finally to the diamine. In addition, after electron transfer, the electron density was distributed on the carboxy groups. Therefore, it can be concluded that the electrons were transferred from the Cu(II) salen complexes to TiO₂.

The electrochemical properties of the complexes **1-9** were determined using cyclic voltammetry (CV) and are presented in Table S6. It can be seen in Figure 4a that the energy level for the conduction band (CB) of TiO₂ was located between that of the LUMOs and HOMOs of the salen Cu dyes. The LUMOs of all the complexes were lower than the CB minimum of TiO₂

(−0.500 V), while the HOMOs of all the complexes were higher than the I₃[−]/I[−] potential of TiO₂ (−0.200 V). Therefore, all the complexes **1-9** should be able to dope electrons in TiO₂ and undergo regeneration. In addition, the electrochemical behaviour of all the complexes **1-9** was reversible; the current values remained unchanged after repeated CV cycles, indicating that no changes in the structures of the complexes occurred. Therefore, it can be concluded that the central Cu metal participated in the redox reactions.

Table S7 summarises the absorption wavelengths, energy levels, redox potentials and calculated HOMO–LUMO gaps for the HOMOs and LUMOs of compounds **1-9**. In addition, the correlation between the π–π* band and the HOMO–LUMO gap is shown in Figure 4b. The relationships between the wavenumbers of the π–π* band and the HOMO–LUMO gap correlated well for both the measured and calculated values obtained *via*

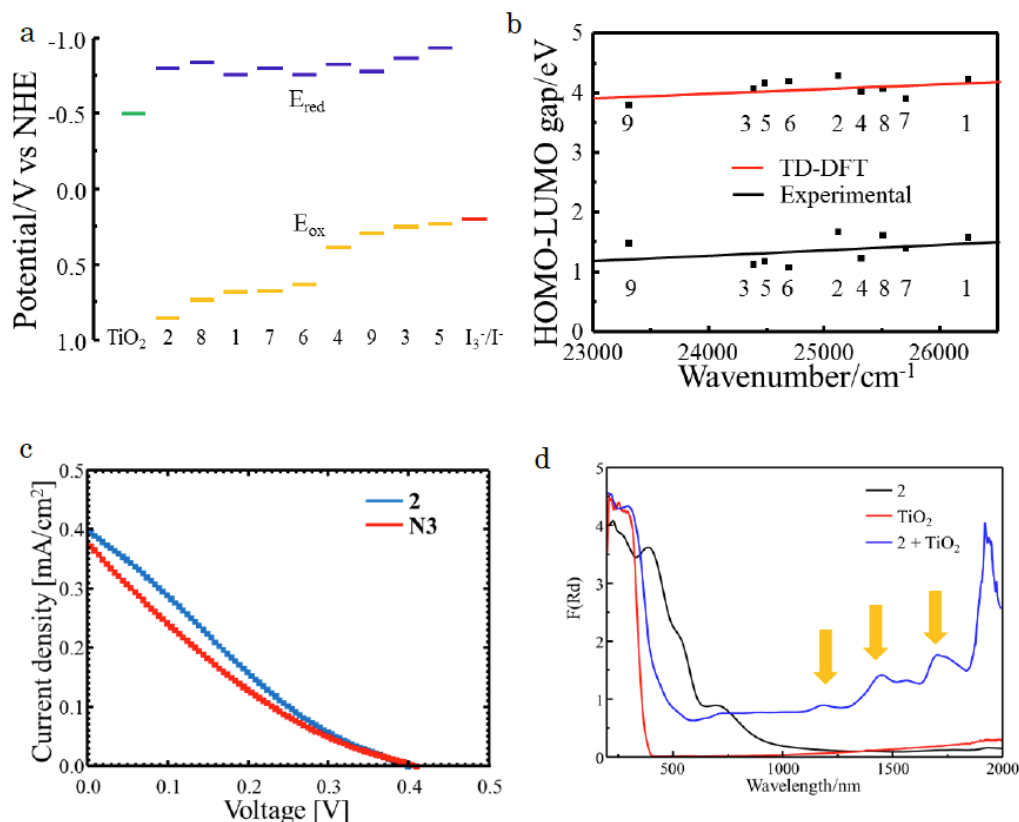


Figure 4: (a) Energy level diagrams for the prepared dyes, TiO_2 and electrolyte, (b) correlation between the values for the π - π^* band and the HOMO-LUMO gap, (c) J - V curves for DSSCs sensitized with **2** and **N3** and (d) absorption wavelength extension because of combining **2** and TiO_2

TD-DFT. In particular, the HOMO-LUMO gap increased as the wavenumber increased. In addition, the central metal did not have a noticeable effect on the differences in the values obtained for the HOMO-LUMO gaps *via* TD-DFT calculations and experimentally. Both the calculated and measured values show a trend due to substituent effects with electron withdrawing groups causing a red-shift, which is in agreement with the results discussed above. Note that all the complexes **1-9** had HOMO-LUMO gaps ≤ 1.65 eV, indicating that they would be suitable as dyes with NIR absorption.

Next, devices were prepared on indium-doped tin oxide (ITO) substrates. A TiO_2 paste made using polyethylene glycol (molecular weight 2000) was coated on ITO using the squeegee method. The TiO_2 film on the ITO glass (active area 2.25 cm^2) was then sintered at 723 K for 1 h. The electrode was immersed immediately in a dye solution (1 mmol/L, DMF:MeOH = 1:9, 24 h) when the oven temperature reached 313 K. The TiO_2 electrode was then removed, flushed with acetonitrile (CH_3CN) and dried under a stream of nitrogen. A solar cell was then fabricated by agglutinating carbon counter and TiO_2 electrodes,

followed by the injection of an electrolyte solution (0.05 M I_2 and 2.0 M LiI in CH_3CN), which penetrated in the TiO_2 film. To investigate the performance of **1**, **2**, **7**, **9** and **N3** in DSSC, test cells were assembled as per literature procedures using an electrolyte composition typically employed for DSSCs based on **N3**. For the present study, the improvement of the performance of well-known types of cells was not a concern; only the performance of the complexes as dyes was investigated. Under identical conditions, the PCEs of complexes **1**, **2**, **7**, **9** and **N3** were $0.6126 \times 10^{-2}\%$, $3.3486 \times 10^{-2}\%$, $0.1690 \times 10^{-2}\%$, $0.7071 \times 10^{-2}\%$ and $3.0609 \times 10^{-2}\%$, respectively. The photovoltaic performance results for DSSCs based on complexes **1**, **2**, **7**, **9** and **N3** are listed in Table S8. The incorporation of an electron withdrawing group at position X- led to an improvement in the J_{sc} value. The J - V curves for the solar cells sensitised using **2** and **N3** are shown in Figure 4c. The change in the J_{sc} value is prominently visible in the power conversion efficiency for **2**, in which the optimisation of the electron transfer process was achieved due the presence of both the electron withdrawing substituent and the inclusion of the carboxy group in the chiral ethylenediamine ligand. In

particular, the LUMO for **2** was close to the conduction band of TiO₂. This adsorption distance between **2** and TiO₂ was optimised by the torsion angle of **2**. Therefore, the contortion of the carboxy group contributed to an increase in the power conversion efficiency. The expansion of the spectral region over which light was absorbed due to the combination of **2** with TiO₂ is shown in Figure 4d. This extension of the wavelengths at which light was absorbed may explain the improved performance of **2**/TiO₂ compared to that of the **N3** dye. The new peaks near 1200 and 1500 nm in the absorption spectrum of **2**/TiO₂ (Figure 4d) may be attributed to dipole interactions or dielectric effects. In addition, the charge transfer peak in the NIR region has been reported to be associated with an increase in interfacial stability following the adsorption of dyes on TiO₂ [19]. It is therefore also thought that the charge transfer peaks in the NIR region (at approximately 1200 and 1500 nm) contributed to the increased power conversion efficiency when **2** was combined with TiO₂. However, the absorbed NIR light was not directly used for photoinduced electron transfer, which occurred via a complicated mechanism (coupling with electron transitions and vibrations). Further investigation is therefore required to clearly elucidate the mechanism. However, it can be concluded that such simple strategy of introducing electron withdrawing groups into well-known salen ligands [20] bound to Cu(II) surely provides complexes with the potential for use as effective and low-cost DSSC dyes.

METHODS

Preparation of 1

To a solution of salicylaldehyde (0.104 g, 1 mmol) dissolved in methanol (10 ml) was added dropwise (2*S*,3*S*)-3-aminoaspartic acid (0.074 g, 0.5 mmol), and the resultant mixture was stirred at 313 K for 2 h to afford a yellow solution of the ligand. Copper(II) acetate monohydrate (0.099 g, 0.5 mmol) was then added, and the solution was stirred for 2 h. Yield 0.255 g (61.1%). *Anal. Calc.*: C, 33.45; H, 4.34 and N, 10.64. Found: C, 33.56; H, 4.28; N, 11.58. IR (KBr, cm⁻¹) 758 (m), 1152 (w), 1310 (w), 1390 (w), 1449 (m), 1604 (s, C=N), 1648 (s, C=O) and 3431 (br, s). T_d: 552.9 K.

Preparation of 2

To a solution of 3,5-dichlorosalicylaldehyde (0.191 g, 1 mmol) dissolved in methanol (10 ml) was added dropwise (2*S*,3*S*)-3-aminoaspartic acid (0.074 g, 0.5 mmol), and the resultant mixture was stirred at 313 K for 2 h to afford a yellow solution of the ligand.

Copper(II) acetate monohydrate (0.099 g, 0.5 mmol) was then added, and the solution was stirred for 2 h. Yield 0.321 g (58.1%). *Anal. Calc.*: C, 33.68; H, 3.26 and N, 7.55. Found: C, 33.62; H, 3.04; N, 7.78. IR (KBr, cm⁻¹) 598 (w), 767 (w), 886 (w), 1153 (m), 1213 (w), 1332 (m), 1391 (m), 1441 (m), 1520 (m), 1627 (s, C=N), 1651 (s, C=O), 2908 (m) and 3433 (br, s). T_d: 531.2 K.

Preparation of 3

To a solution of 3,5-dibromosalicylaldehyde (0.4086 g, 1 mmol) dissolved in methanol (10 ml) was added dropwise (2*S*,3*S*)-3-aminoaspartic acid (0.074 g, 0.5 mmol), and the resultant mixture was stirred at 313 K for 2 h to afford a yellow solution of the ligand. Copper(II) acetate monohydrate (0.099 g, 0.5 mmol) was then added, and the solution was stirred for 2 h. Yield 0.203 g (55.5%). *Anal. Calc.*: C, 27.50; H, 2.31 and N, 4.58. Found: C, 27.79; H, 2.28; N, 4.92. IR (KBr, cm⁻¹) 592 (w), 720 (w), 754 (w), 883 (w), 1147 (s), 1216 (m), 1330 (m), 1415 (m), 1439 (m), 1502 (m), 1619 (s, C=N), 1648 (s, C=O), 3052 (w), 3332 (w) and 3446 (br, s). T_d: 622.2 K.

Preparation of 4

To a solution of 3,5-di-tert-butylsalicylaldehyde (0.234 g, 1 mmol) dissolved in methanol (10 ml) was added dropwise (2*S*,3*S*)-3-aminoaspartic acid (0.074 g, 0.5 mmol), and the resultant mixture was stirred at 313 K for 2 h to afford a yellow solution of the ligand. Copper(II) acetate monohydrate (0.099 g, 0.5 mmol) was then added, and the solution was stirred for 2 h. Yield 0.352 g (54.9%). *Anal. Calc.*: C, 38.36; H, 3.08 and N, 5.84. Found: C, 38.48; H, 2.95; N, 5.58. IR (KBr, cm⁻¹) 591 (w), 729 (w), 1027 (w), 1165 (m), 1265 (w), 1384 (m), 1532 (m), 1619 (s, C=N), 1653 (s, C=O), 2960 (m) and 3435 (br, s). T_d: 539.1 K.

Preparation of 5

To a solution of *O*-vanilin (0.129 g, 1 mmol) dissolved in methanol (10 ml) was added dropwise (2*S*,3*S*)-3-aminoaspartic acid (0.074 g, 0.5 mmol), and the resultant mixture was stirred at 313 K for 2 h to afford a yellow solution of the ligand. Copper(II) acetate monohydrate (0.099 g, 0.5 mmol) was then added, and the solution was stirred for 2 h. Yield 0.210 g (42.8%). *Anal. Calc.*: C, 42.34; H, 3.74 and N, 5.20. Found: C, 42.38; H, 3.63; N, 5.11. IR (KBr, cm⁻¹) 617(w), 667 (w), 746 (w), 855 (w), 1147 (s), 1216 (m), 1330 (m), 1415 (m), 1439 (m), 1502 (m), 1604 (m), 1623 (s, C=N), 1707 (s, C=O), 3052 (w), 3332 (w) and 3446 (br, s). T_d: 530.5 K.

Preparation of 6

To a solution of 2,3-dihydroxybenzaldehyde (0.138 g, 1 mmol) dissolved in methanol (10 ml), (2*S*,3*S*)-3-Aminoaspartic acid (0.074 g, 0.5mmol) was added dropwise and stirred at 313 K for 2 h to give a yellow solution of the ligand. Copper(II) acetate monohydrate (0.099 g, 0.5 mmol) were added and stirred for 2 h.

Yield 0.251 g (55.7 %). *Anal.* Calc.: C, 42.34; H, 3.74; N, 5.20. Found: C, 42.38; H, 3.63; N, 5.11. IR (KBr, cm^{-1}) 642 (w), 860 (w), 1128 (m), 1197 (w), 1237 (s), 1386 (m), 1435 (m), 1564 (m), 1623 (s, C=N), 1707 (s, C=O), 2856 (w), 2925 (m), 3431 (br, s). T_d : 544.9 K.

Preparation of 7

To a solution of 5-chlorosalicylaldehyde (0.156 g, 1 mmol) dissolved in methanol (10 ml), (2*S*,3*S*)-3-Aminoaspartic acid (0.074 g, 0.5mmol) was added dropwise and stirred at 313 K for 2 h to give a yellow solution of the ligand. Copper(II) acetate monohydrate (0.099 g, 0.5 mmol) were added and stirred for 2 h.

Yield 0.343 g (70.6 %). *Anal.* Calc.: C, 38.36; H, 3.08; N, 5.84. Found: C, 38.48; H, 2.95; N, 5.58. IR (KBr, cm^{-1}) 661 (w), 829 (w), 1156 (w), 1493 (m), 1623 (s, C=N), 1683 (s, C=O), 2237 (w), 2921 (w), 2921 (w), 3456 (br, s). T_d : 549.7 K.

Preparation of 8

To a solution of 5-bromosalicylaldehyde (0.2934 g, 1 mmol) dissolved in methanol (10 ml), (2*S*,3*S*)-3-Aminoaspartic acid (0.074 g, 0.5mmol) was added dropwise and stirred at 313 K for 2 h to give a yellow solution of the ligand. Copper(II) acetate monohydrate (0.099 g, 0.5 mmol) were added and stirred for 2 h.

Yield 0.134 g (46.5 %). *Anal.* Calc.: C, 32.27; H, 1.81; N, 4.18. Found: C, 32.65; H, 1.91; N, 4.18. IR (KBr, cm^{-1}) 542 (w), 611 (w), 649 (w), 706 (w), 800 (w), 834 (m), 894 (w), 944 (w), 944 (w), 1073 (w), 1186 (m), 1273 (s), 1368 (s), 1468 (m), 1536 (m), 1606 (s, C=N), 1652 (s, C=O), 2943 (w), 3092 (w), 3429 (br, s). T_d : 568.4 K.

Preparation of 9

To a solution of 2-hydroxy-5-methoxybenzaldehyde (0.124 g, 1 mmol) dissolved in methanol (10 ml), (2*S*,3*S*)-3-Aminoaspartic acid (0.074 g, 0.5mmol) was added dropwise and stirred at 313 K for 2 h to give a yellow solution of the ligand. Copper(II) acetate monohydrate (0.099 g, 0.5 mmol) were added and stirred for 2 h.

Yield 0.307 g (64.3 %). *Anal.* Calc.: C, 37.91; H, 3.89; N, 8.19. Found: C, 37.69; H, 3.77; N, 8.48. IR (KBr, cm^{-1}) 591 (w), 809 (w), 1027 (w), 1116 (w), 1165 (w), 1294 (m), 1384 (m), 1384 (m), 1473 (w), 1611 (C=N), 1647 (C=O), 2920 (w), 3435 (br, s). T_d : 543.0 K.

X-Ray Crystallography

The powder X-ray diffraction patterns of complexes **1**, **2**, **4** and **6** were obtained at 298 K on a Rigaku Smart Lab system at the University of Tokyo. Structural analyses were performed using the Rietveld method [S3] and PDXL2 ver.2.2.1.0 (Rigaku Corporation). Although **1**, **2**, **4** and **6** are chiral molecules, they are solved as space group $P2_1/n$ to indicate reasonable density because of uncertain systematic absence of powder diffraction.

Computation

All calculations were performed using the Gaussian 09W software Revision A.02 (Gaussian, Inc.). The gas-phase geometry optimisations were performed using TD-DFT with the B3LYP functional. The vertical excitation energies were calculated using the LanL2DZ method for Cu with the 6-31+G(d) basis set for H, C, N, O, Cl and Br and based on the singlet ground-state geometry.

Measurements

Elemental analyses (C, H and N) were performed using a Perkin-Elmer 2400 II CHNS/O analyser at the Tokyo University of Science. IR spectra were recorded as KBr pellets on a JASCO FT-IR 4200 plus spectrophotometer in the range 4000–400 cm^{-1} at 298 K. Absorption spectra were obtained on a JASCO V-570 UV-vis-NIR spectrophotometer in the range 2000–200 nm at 298 K. CD spectra were obtained on a JASCO J-820 spectropolarimeter in the range 900–250 nm at 298 K. TG-DTA profiles were obtained in air at a heating rate of 10 Kmin^{-1} using a Rigaku TG8120. CV curves were obtained via BAS AIS/DY2323 using a traditional three-electrode system. The working, reference and auxiliary electrodes were a Pt disk, Ag/AgCl and Pt wire, respectively. The performance of DSSCs was determined from J - V curves obtained under air mass 1.5 conditions at an illumination of 100 mW/cm^2 using an ADCMT 6241A DC voltage/current source/monitor. All measurements were performed at room temperature.

